Partially composite Higgs models: Phenomenology and RG analysis

Tommi Alanne[a] **Diogo Buarque Franzosi**[b] **Mads T. Frandsen**[c] **Mette L.A. Kristensen**[c] **Aurora Meroni**[d] **Martin Rosenlyst**[c]

[a] *Max-Planck-Institut für Kernphysik, Saupfercheckweg 1, 69117 Heidelberg, Germany*

[b] *Institut für Theoretische Physik, Universität Göttingen, Friedrich-Hund-Platz 1, 37077 Göttingen, Germany*

[c] *CP³-Origins, University of Southern Denmark, Campusvej 55, DK-5230 Odense M, Denmark*

[d] *Department of Physics, University of Helsinki, & Helsinki Institute of Physics, P.O.Box 64, FI-00014 University of Helsinki, Finland*

E-mail: tommi.alanne@mpi-hd.mpg.de, dbuarqu@gwdg.de, frandsen@cp3.sdu.dk, metkr03@student.sdu.dk, aurora.meroni@helsinki.fi, rosenlyst@cp3.sdu.dk

ABSTRACT:
We study the phenomenology of partially composite-Higgs models where electroweak symmetry breaking is dynamically induced, and the Higgs is a mixture of a composite and an elementary state. The models considered have explicit realizations in terms of gauge-Yukawa theories with new strongly interacting fermions coupled to elementary scalars and allow for a very SM-like Higgs state. We study constraints on their parameter spaces from vacuum stability and perturbativity as well as from LHC results and find that requiring vacuum stability up to the compositeness scale already imposes relevant constraints. A small part of parameter space around the classically conformal limit is stable up to the Planck scale. This is however already strongly disfavored by LHC results. In different limits, the models realize both (partially) composite-Higgs and (bosonic) technicolor models and a dynamical extension of the fundamental Goldstone-Higgs model. Therefore, they provide a general framework for exploring the phenomenology of composite dynamics.

Contents

1 Introduction

Partially composite-Higgs (CH) models with underlying four-dimensional realizations in terms of new fermions coupled to elementary scalar multiplets via Yukawa interactions [1] were recently developed and studied in Refs. [2–5]. These models feature dynamically induced electroweak symmetry breaking (EWSB) and a partially composite pseudo-Goldstone boson (pGB) Higgs. The elementary scalar multiplet provides masses for the SM fermions via SM-like Yukawa interactions [6] avoiding the complications of fermion partial compositeness [7] or extended-technicolor-type constructions [8–10]. The framework gives a unified description for various classes of models from (partially) CH [1] to (bosonic) technicolor (b)TC [11, 12].

However, such models may suffer from a low vacuum instability scale due to the enhancement of the top Yukawa coupling of the Higgs state as compared to the SM Higgs [13]. In this paper we, therefore, study the vacuum stability and perturbativity bounds on the parameter space of minimal partially CH (pCH) models [2, 3, 5] and combine these self-consistency conditions with current constraints from collider experiments. We show that even the requirement of stability up to the compositeness scale provides relevant constraints regardless of the particular UV realization. We also consider model extensions where a (small) part of the top-quark mass does not originate from the vacuum expectation value (vev) of the elementary scalar multiplet as a possibility to alleviate the vacuum-stability bounds.

The two underlying concrete models we consider both consist of four Weyl fermions, $U_{L,R}, D_{L,R}$, transforming under a new $SU(2)_{TC}$ gauge group with the left-handed components forming a doublet, (U_L, D_L), under the weak gauge group $SU(2)_w$. This is the minimal CH model with four-dimensional fermionic realisation [14], and the new fermion sector features an enhanced $SU(4)$ global symmetry acting on the four Weyl fermions. The fermions are coupled to a multiplet of new elementary scalars via Yukawa interactions, and the dynamical condensation of the strongly interacting (techni)fermions is transmitted to the scalar multiplet via these Yukawa interactions. As a consequence, the fundamental scalar multiplet acquires a vev. We begin by considering a $SU(2)_w$ doublet of scalars [2, 3] and then study a full multiplet under the global $SU(4)$ symmetry of the new fermion sector [5].

While the SM fermions obtain their masses via the vev of the elementary scalar multiplet, the weak boson masses originate from both the vev and the condensate in the composite sector. Consequently, the electroweak (EW) scale is given by

$$v_w^2 = v^2 + f^2 \sin^2\theta, \tag{1.1}$$

where $v_w = 246$ GeV, we denote the vev of the neutral CP-even component of the elementary Higgs by v, f is the Goldstone-boson decay constant of the composite sector, and θ ($\pi/2 \le \theta \le \pi$) parameterises the vacuum misalignment.

2 Minimal partially composite Higgs models

We consider here the minimal four-dimensional strongly interacting fermionic sector allowing for a composite Goldstone Higgs boson. This is based on the gauge group $SU(2)_{TC}$ and contains four Weyl fermions transforming in the fundamental representation of the gauge group. The new fermion sector in isolation features a global $SU(4)$ symmetry, which upon condensation breaks spontaneously to $Sp(4)$ [15]. The left-handed fermions (U_L, D_L) transform as a doublet under $SU(2)_w$, and the EW gauge group can be embedded into the $SU(4)$ global symmetry via the left and right generators

$$T_L^i = \frac{1}{2}\begin{pmatrix} \sigma_i & 0 \\ 0 & 0 \end{pmatrix}, \; T_R^i = \frac{1}{2}\begin{pmatrix} 0 & 0 \\ 0 & -\sigma_i^T \end{pmatrix}. \tag{2.1}$$

The T_L generators may be identified with those of the $SU(2)_w$ and T_R^3 with the generator of hypercharge [16–19]. The five Goldstone bosons (GBs) associated to the breaking $SU(4) \rightarrow Sp(4)$ then form an EW doublet and a singlet. We list the left-handed fermions and their quantum numbers using the notation $\widetilde{U}_L \equiv \epsilon U_R^*$ in Tab. 1. The details of the construction of the effective description can be found e.g. in Refs. [2, 5].

Table 1: New fermion content.

	$SU(2)_{TC}$	$SU(2)_W$	$U(1)_Y$
Q_L	$\square$	$\square$	0
$\widetilde{U}_L$	$\square$	1	$-1/2$
$\widetilde{D}_L$	$\square$	1	$+1/2$

There are different possibilities to align the stability group, $Sp(4)$, with respect to the EW gauge symmetry inside the $SU(4)$. In particular, the EW group can be embedded completely within the stability group leading to unbroken EW symmetry. There are two inequivalent vacua, $E_\pm$, corresponding to this orientation. On the other hand, it is possible that only the electromagnetic subgroup, $U(1)_Q$, is unbroken as in TC models [20, 21]. We denote the corresponding vacuum by E_B. The different vacua can be represented as the matrices

$$E_\pm = \begin{pmatrix} i\sigma_2 & 0 \\ 0 & \pm i\sigma_2 \end{pmatrix}, \qquad E_B = \begin{pmatrix} 0 & 1 \\ -1 & 0 \end{pmatrix}. \tag{2.2}$$

In general, the vacuum is a superposition of an EW-preserving and the EW-breaking vacua, and can be written as

$$E = \cos\theta E_- + \sin\theta E_B. \tag{2.3}$$

The misalignment angle, θ, is determined by the sources of explicit $SU(4)$ breaking, and the relation between the composite scale and the EW scale is then given in terms of θ according to Eq. (1.1).

We parameterise the composite Goldstone-boson degrees of freedom in the $SU(4)/Sp(4)$ coset by

$$\Sigma = \exp\left(\frac{2\sqrt{2}\,i}{f}\Pi^a X^a\right) E, \tag{2.4}$$

where the broken generators, X^a, with $a = 1, \ldots, 5$, correspond to the vacuum E. The generators are explicitly given in Ref. [17]. Furthermore, we introduce spurions, $P_\alpha, \widetilde{P}_\alpha$, such that $\mathrm{Tr}[P_\alpha\Sigma]$ and $\mathrm{Tr}[\widetilde{P}_\alpha\Sigma]$ transform as EW doublets with hypercharges $+1/2$ and $-1/2$, respectively. These can be explicitly written as

$$\begin{aligned}
2P_1 &= \delta_{i1}\delta_{j3} - \delta_{i3}\delta_{j1}, \quad 2P_2 = \delta_{i2}\delta_{j3} - \delta_{i3}\delta_{j2}, \\
2\widetilde{P}_1 &= \delta_{i1}\delta_{j4} - \delta_{i4}\delta_{j1}, \quad 2\widetilde{P}_2 = \delta_{i2}\delta_{j4} - \delta_{i4}\delta_{j2}.
\end{aligned} \tag{2.5}$$

2.1 Model I: Elementary scalar doublet

In addition to the composite pions, Σ, we introduce an (elementary) scalar multiplet. We begin by considering an $SU(2)_L$ doublet, H_α, and we also introduce vector-like masses for

the new fermions [2, 3] via the matrix M:

$$H_\alpha = \frac{1}{\sqrt{2}} \begin{pmatrix} \sigma_h - \mathrm{i}\pi_h^3 \\ -(\pi_h^2 + \mathrm{i}\pi_h^1) \end{pmatrix}, \quad M = \begin{pmatrix} m_1\epsilon & 0 \\ 0 & -m_2\epsilon \end{pmatrix}. \tag{2.6}$$

With this field content, the underlying Lagrangian describing the new strong sector and the elementary doublet can be written as

$$\begin{aligned} \mathcal{L}_{\mathrm{pCH}} =& \bar{Q}\mathrm{i}\slashed{D}Q + D_\mu H^\dagger D^\mu H - m_H^2 H^\dagger H - \lambda_H (H^\dagger H)^2 \\ &+ \frac{1}{2}Q^T M Q - y_U H_\alpha (Q^T P_\alpha Q) - y_D \widetilde{H}_\alpha (Q^T \widetilde{P}_\alpha Q) + \mathrm{h.c.}, \end{aligned} \tag{2.7}$$

where $Q = (U_\mathrm{L}, D_\mathrm{L}, \widetilde{U}_\mathrm{L}, \widetilde{D}_\mathrm{L})$, $\widetilde{H} = \epsilon H^*$, and the antisymmetric contractions are kept implicit. The global SU(4) symmetry of the composite sector is in this case broken explicitly to $\mathrm{SU}(2)_\mathrm{w} \times \mathrm{U}(1)_Y$ by both the Yukawa and weak interactions, and the vector like masses in M. The Yukawa couplings with the SM fermions, restricting to the third generation of SM quarks, are

$$\mathcal{L}_{\mathrm{Yuk}} = -y_t \bar{q}_\mathrm{L} H t_\mathrm{R} - y_b \bar{q}_\mathrm{L} \widetilde{H} b_\mathrm{R} + \mathrm{h.c.}, \tag{2.8}$$

where $q_L = (t_L, b_L)$. This model was considered in Refs. [2, 3] in the limit $\lambda_H = 0$ but here we keep λ_H throughout, since it is relevant for the vacuum stability, and since we do not assume necessarily any supersymmetric completion that would alter the running of λ_H at high energies.

Below the condensation scale, $\Lambda_{\mathrm{TC}} \sim 4\pi f$, Eq. (2.7) yields the following lowest-order effective potential

$$\begin{aligned} V_{\mathrm{eff}}^0 =& 4\pi f^3 Z_2 \left(\frac{1}{2}\mathrm{Tr}\,[M\Sigma] + y_U H_\alpha \mathrm{Tr}\,[P_\alpha \Sigma] + y_D \widetilde{H}_\alpha \mathrm{Tr}[\widetilde{P}_\alpha \Sigma] + \mathrm{h.c.} \right) \\ &+ m_H^2 H^\dagger H + \lambda_H (H^\dagger H)^2, \end{aligned} \tag{2.9}$$

where Z_2 is a non-perturbative $\mathcal{O}(1)$ constant, and we use the numerical value $Z_2 \approx 1.5$ suggested by the lattice simulations [1] [22]. The EW gauge interactions contribute to the effective potential at the one-loop level, but the contribution is subleading as compared to the vector-like mass terms. It is, however, important for the model we describe in the next section.

2.2 Model II: SU(4) completion of the scalar sector

A model retaining the global SU(4) symmetry on the new fermion sector in the presence of the Yukawa interactions was proposed in Ref. [5]. The elementary scalar doublet is extended to a complete two-index antisymmetric SU(4) representation, Φ, allowing for the Yukawa interactions of the elementary scalars and the new fermions to remain SU(4) symmetric. Furthermore, the vector-like masses, $m_{1,2}$, of the new fermions above are then generated via the dynamically induced vev of the EW-singlet component of the scalar multiplet, Φ. The misalignment of the vacuum, $\theta \neq 0$, required to give a mass to the would-be pGB Higgs boson may come solely from the SM sector and the scalar potential. In the following, we briefly outline the model and the construction of the effective low-energy Lagrangian, but we refer to Ref. [5] for details.

The scalar multiplet, Φ, can be conveniently parameterised in terms of the EW eigenstates. To this end, we write $H_\alpha \equiv \mathrm{Tr}[P_\alpha \Phi]$ and $\widetilde{H}_\alpha \equiv \mathrm{Tr}[\widetilde{P}_\alpha \Phi]$ that transform as EW

---

[1]Ref. [22] gives $\langle Q^T Q \rangle^{1/3}/f = 4.19(26)$ for the condensate, which then yields an estimate (with a factor 4 accounting for the trace): $Z_2 = \frac{1}{4 \cdot 4\pi} \left(\frac{\langle Q^T Q \rangle^{1/3}}{f} \right)^3 \approx 1.5$.

doublets with hypercharges $+1/2$ and $-1/2$, respectively. The EW-singlet directions can be projected out with the following spurions:

$$P_1^{\mathrm{S}} = \frac{1}{2} \begin{pmatrix} -\mathrm{i}\sigma_2 & 0 \\ 0 & 0 \end{pmatrix}, \ P_2^{\mathrm{S}} = \frac{1}{2} \begin{pmatrix} 0 & 0 \\ 0 & \mathrm{i}\sigma_2 \end{pmatrix}. \tag{2.10}$$

Thus, we arrive at

$$\Phi = \sum_{\alpha=1,2} P_\alpha H_\alpha + \widetilde{P}_\alpha \widetilde{H}_\alpha + P_1^{\mathrm{S}} S + P_2^{\mathrm{S}} S^*, \tag{2.11}$$

where H is given in Eq. (2.6), and $S = \frac{1}{\sqrt{2}}(S_{\mathrm{R}} + \mathrm{i}S_{\mathrm{I}})$ parameterises the EW-singlet scalars. The relevant Lagrangian, restricting to third generation of SM quarks, is then

$$\begin{aligned}
\mathcal{L}_{\mathrm{pCH}_2} =& \bar{Q}\mathrm{i}\slashed{D}Q + \mathrm{Tr}[D_\mu \Phi^\dagger D^\mu \Phi] - m_\Phi^2 \mathrm{Tr}[\Phi^\dagger \Phi] - \lambda_\Phi \mathrm{Tr}[\Phi^\dagger \Phi]^2 \\
& - y_Q Q^T \Phi Q - y_t \bar{q}_{\mathrm{L}} H t_{\mathrm{R}} - y_b \bar{q}_{\mathrm{L}} \widetilde{H} b_{\mathrm{R}} + \mathrm{h.c.}
\end{aligned} \tag{2.12}$$

Below the condensation scale, we have the lowest-order effective potential

$$V_{\mathrm{eff}}^0 = 4\pi f^3 Z_2 \left(y_Q \mathrm{Tr}\left[\Phi\Sigma\right] + \ \mathrm{h.c.}\right) + m_\Phi^2 \mathrm{Tr}[\Phi^\dagger \Phi] + \lambda_\Phi \mathrm{Tr}[\Phi^\dagger \Phi]^2. \tag{2.13}$$

At this level, the global symmetry is broken only spontaneously by the condensation in the strong sector. Therefore, in order to misalign the vacuum with respect to EW symmetry and to give a mass to one of the GB's to be identified with the Higgs, we need to consider sources that break the global symmetry explicitly. To this end, we include the leading EW contribution in the effective potential [23, 24]

$$V_{\mathrm{gauge}} = - C_g \left[g^2 f^4 \sum_{i=1}^{3} \mathrm{Tr}\left(T_{\mathrm{L}}^i \Sigma (T_{\mathrm{L}}^i \Sigma)^*\right) + g'^{\,2} f^4 \mathrm{Tr}\left(T_{\mathrm{R}}^3 \Sigma (T_{\mathrm{R}}^3 \Sigma)^*\right)\right], \tag{2.14}$$

where C_g is a positive $\mathcal{O}(1)$ loop factor. Differently from Ref. [18], the top quark interactions are subleading in the vacuum determination, since the top quark only couples to the weakly interacting fundamental sector. We add another source of explicit breaking of the global symmetry by splitting of the masses of the EW-doublet and singlet components of the scalar multiplet, Φ:

$$V_{\delta m^2} = 2\delta m^2 \, \mathrm{Tr}[P_i^S \Phi]\mathrm{Tr}[P_i^S \Phi]^* = \frac{1}{2}\delta m^2 (S_{\mathrm{R}}^2 + S_{\mathrm{I}}^2). \tag{2.15}$$

As shown in Ref. [5], these two sources are enough to achieve a non-trivial vacuum alignment, and therefore we need not introduce further explicit breaking sources directly on the new fermion sector.

3 Model I: RG analysis and phenomenological constraints

3.1 Vacuum, spectrum, and λ_H

The effective potential of Eq. (2.9) as a function of σ_h and θ reads

$$V_{\mathrm{eff}} = 8\pi f^3 Z_2 \left(m_{12} c_\theta - \frac{y_{UD}}{\sqrt{2}}\sigma_h s_\theta\right) + \frac{1}{2}m_H^2 \sigma_h^2 + \frac{\lambda_H}{4}\sigma_h^4, \tag{3.1}$$

where $m_{12} \equiv m_1 + m_2$ and $y_{UD} \equiv y_U + y_D$. We use the short-hand notations $s_x \equiv \sin x$, $c_x \equiv \cos x$, and $t_x \equiv \tan x$. Further, we define the parameter $m_\lambda^2 \equiv m_H^2 + \lambda_H v^2$, the form factor $F_0 = 4\pi Z_2$ and trade v for the angle β via

$$t_\beta \equiv \frac{v}{f s_\theta}. \tag{3.2}$$

The vacuum conditions then read

$$\begin{aligned}
0 &= \left.\frac{\partial V_{\text{eff}}}{\partial \sigma_h}\right|_{\sigma_h=v} = -\sqrt{2}F_0 y_{UD} f^3 s_\theta + m_\lambda^2 v, \\
0 &= \left.\frac{\partial V_{\text{eff}}}{\partial \theta}\right|_{\sigma_h=v} = -2F_0 f^3 \left(m_{12} s_\theta + \frac{y_{UD}}{\sqrt{2}} v c_\theta\right).
\end{aligned} \tag{3.3}$$

These yield the parameter constraint equations

$$y_{UD} = \frac{t_\beta m_\lambda^2}{\sqrt{2} f^2 F_0}, \quad m_{12} = -\frac{c_\theta m_\lambda^2 t_\beta^2}{2 F_0 f}. \tag{3.4}$$

For $t_\beta \gtrsim 1$, the first equation limits the mass parameter to $m_H^2 \lesssim 4\pi f^2$ as long as $y_{UD} \lesssim 1$. If the latter limit on y_{UD} is not satisfied, then these large Yukawa couplings will drive the scalar quartic negative at very low scales. Indeed we find that $y_{UD} \ll 1$ for all the viable parameter space that we consider, and this condition is thus automatically satisfied.

The model features seven parameters relevant to our study, [2] y_{UD}, m_{12}, λ_H, s_θ, t_β, f, m_H^2, and four constraint equations including the two vacuum conditions in Eq. (3.3), the EW scale Eq. (1.1), and the Higgs mass, whose expression is shown below in Eq. (3.9). We take s_θ, t_β and m_H^2 as free parameters.

The Yukawa coupling between the top quark and the elementary doublet is enhanced with respect to the SM value by

$$y_t = y_t^{\text{SM}}/s_\beta. \tag{3.5}$$

For a given value of the quartic coupling, λ_H, in Eq. (2.7), this implies a lower limit on t_β in order to avoid vacuum instability above the EWSB scale and below the Planck scale. We discuss this issue in detail in Sec. 3.2.

The charged pion and neutral CP-even scalar mass matrices, in the bases (π_h^+, Π^+), (σ_h, Π^4), resp., can be written as

$$M_{\pi^+}^2 = m_\lambda^2 \begin{pmatrix} 1 & t_\beta \\ t_\beta & t_\beta^2 \end{pmatrix}, \quad M_h^2 = m_\lambda^2 \begin{pmatrix} 1+\delta & -c_\theta t_\beta \\ -c_\theta t_\beta & t_\beta^2 \end{pmatrix}, \tag{3.6}$$

where $\delta \equiv 2\frac{\lambda_H v^2}{m_\lambda^2}$. The mass of the heavy neutral pion, π^0, coincides with the mass of the charged ones.

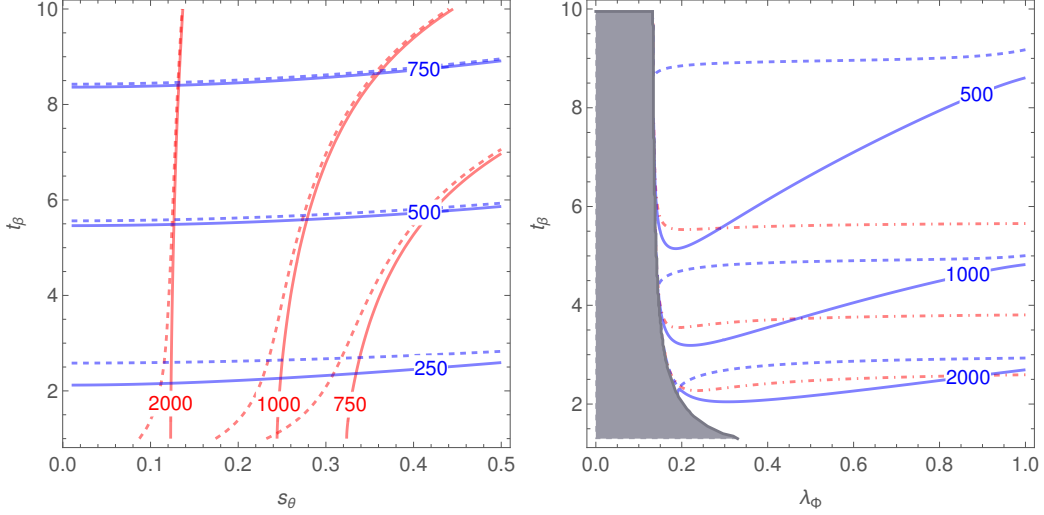The CP-even mass eigenstates are given in terms of the interaction eigenstates by

$$h_1 = c_\alpha \sigma_h - s_\alpha \Pi^4, \quad h_2 = s_\alpha \sigma_h + c_\alpha \Pi^4, \tag{3.7}$$

with

$$t_{2\alpha} = \frac{2 t_\beta c_\theta}{1 - t_\beta^2 + \delta}. \tag{3.8}$$

---

[2] Only the combinations m_{12} and y_{UD} enter into the vacuum equations and the effect of y_U, y_D on the running of the couplings is negligible in the parameter space considered.

Figure 1: **Left panel:** Model I spectrum. The blue (red) solid contours show the mass of the heavier CP-even state, $\mathcal{H}$, in GeV for fixed $m_H^2/f^2 = 0$ ($m_H^2/f^2 = 1$). The dashed curves show the mass of the pseudoscalar Π_5 for the same scenarios. **Right panel:** Model II spectrum. The solid (dashed) blue lines show the mass contours (500 GeV, 1000 GeV, 2000 GeV) of m_{h_2} (m_{h_3}). The mass of the heavy pion triplet follows closely the contours of m_{h_3}, and we have omitted those for clarity. The dot-dashed red lines show the same mass contours for the non-pGB mass eigenstate of the two mixing pseudoscalar states, Π_5 and $S_{\rm I}$. We have fixed $s_\theta = 0.1$.

The corresponding masses of the neutral and charged eigenstates are

$$m_{h_{1,2}}^2 = \frac{m_\lambda^2}{2} \left[1 + t_\beta^2 + \delta \pm \left(2c_\theta t_\beta s_{2\alpha} + (1 - t_\beta^2 + \delta)c_{2\alpha} \right) \right],$$
$$m_{\pi^\pm,0}^2 = m_\lambda^2/c_\beta^2, \quad m_{\Pi_5}^2 = t_\beta^2 m_\lambda^2.$$
(3.9)

Using Eq. (3.8) and expanding in s_θ^2 and t_β^{-2}, we then find

$$m_{h_1}^2 \simeq m_\lambda^2 \left(s_\theta^2 + (1 - t_\beta^{-2})\delta \right), \quad m_{h_2}^2 \simeq m_\lambda^2 \left(1 + t_\beta^2 \right), \quad m_{\pi^\pm,0}^2 = m_\lambda^2 \left(1 + t_\beta^2 \right). \tag{3.10}$$

We now identify the lightest of the neutral CP-even eigenstates with the 125-GeV Higgs boson. In most of parameter space this is the h_1 state, but for $1 + \delta > t_\beta^2$ it is instead h_2 as seen from Eq. (3.6). We denote the heavier CP-even eigenstate by $\mathcal{H}$.

We show the mass of $\mathcal{H}$ for fixed $m_H^2/f^2 = 0, 1$ in the (s_θ, t_β) plane in the left panel of Fig 1. The simple scaling of the heavy masses with t_β, roughly independent of s_θ, is apparent in the $m_H^2/f^2 = 0$ case (blue lines). Instead the dependence on s_θ in the case $m_H^2/f^2 = 1$ (red dotted lines) follows from the vev condition Eq. (1.1) implying the scaling $m_\lambda^2 \simeq m_H^2 \simeq v_{\rm EW}^2 s_\theta^{-2} t_\beta^{-2}$ which cancels the t_β^2 factor in the heavy mass formulas. The mass of the heavy pion triplet nearly coincides with the mass of the heavier CP-even state for the parameters we consider, and we have omitted that for clarity in the plot.

Using the experimental value of the Higgs mass and fixing the mass parameter to $m_H^2 = 0$ ($m_H^2 = f^2$), we show on the left panel of Fig. 2 with blue (yellow) contours the value of λ_H in (s_θ, t_β) plane. The figure demonstrates that the value of λ_H may only be increased slightly beyond its value in the SM $\lambda_{\rm SM} \approx 0.129$ unless t_β is very small.
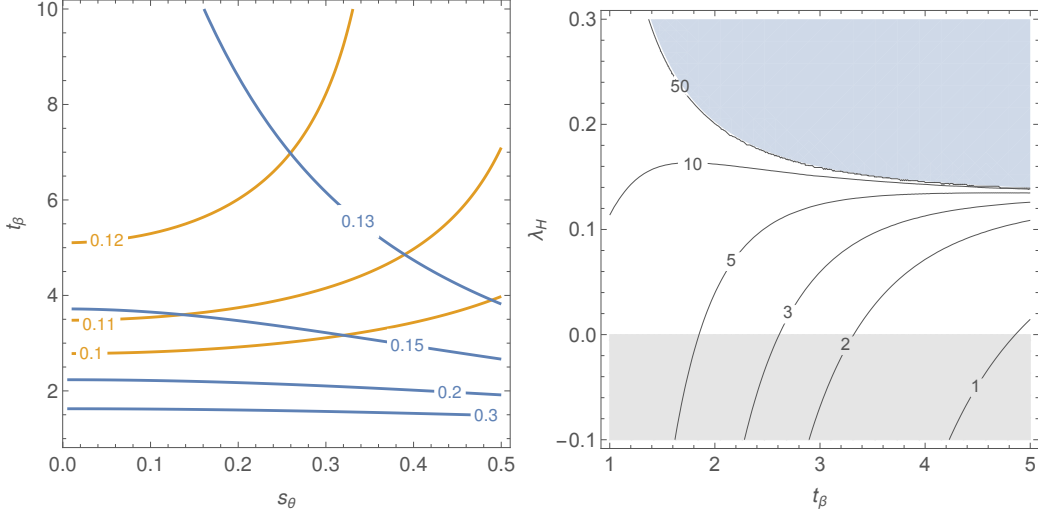
Figure 2: **Left panel:** Values of λ_H. Blue (yellow) contours represent the case $m_H^2/f^2 = 0$ ($m_H^2/f^2 = 1$). **Right panel:** The contours show the value of $\Lambda_{\text{TC}} = 4\pi f$ in TeV corresponding to a 1 TeV heavy Higgs mass. The region $\lambda_H < 0$ is excluded by the requirement of stability of the potential. For $\Lambda_{\text{TC}} \to \infty$ the curves lie on top of the $\Lambda_{\text{TC}} = 50$ TeV contour so the shaded area results in no viable solutions. More details in the text.

Since for large t_β, the light Higgs mass is a sum of two manifestly positive contributions, cf. Eq. (3.10), the scalar quartic coupling is bounded for a given value of t_β to $\lambda_H \lesssim \lambda_{\text{SM}}/s_\beta^2$, and the bound is only reached in the limit $m_H^2 \to 0, s_\theta \to 0$. Furthermore, for $t_\beta \to \infty$, this bound reduces to the SM value. On the right panel of Fig. 2, we show the contour lines in the (t_β, λ_H) plane for different values of $\Lambda_{\text{TC}} = 4\pi f$ in TeV having fixed the Higgs mass, and the mass of the heavier eigenstate to 1 TeV for concreteness. In the lower shaded region, $\lambda_H < 0$ and this is excluded due to vacuum instability. The boundary of the upper blue shaded region shows the maximum allowed value of λ_H for which the correct Higgs mass can still be achieved as a function of t_β. The $\Lambda_{\text{TC}} \to \infty$ contours lie very close to the $\Lambda_{\text{TC}} = 50$ TeV contour. This boundary is almost independent of the fixed value of the heavy eigenstate mass, and the blue shaded region is thus inaccessible.

The accessible values of λ_H shown in Fig. 2, together with the enhanced top Yukawa in Eq. (3.5), make it clear that it is important to consider the vacuum stability constraints on the model.

3.2 RG analysis and vacuum stability

The running of λ_H is driven dominantly by the top loop, as in the SM. However, compared to the SM, the top Yukawa coupling of the elementary interaction eigenstate, σ_h, is enhanced by $y_t = y_t^{\text{SM}}/s_\beta$. Therefore λ_H will run negative faster than in the SM for the same weak scale initial value, and the vacuum of the model will, thus, not be stable in all of parameter space. The problem is similar to that in bTC [13] and in type-I two-Higgs-doublet models (2HDM).

In Appendix A, we tabulate the one-loop beta functions for the bTC/pCH framework with N_F new $SU(2)_L$-doublet fermionic fields, $Q_L = (U_L, D_L)$, transforming under the representation R_F of the new strong gauge group. These fields will couple to the elementary Higgs doublet, H, through Yukawa-like interactions with couplings y_U and y_D.
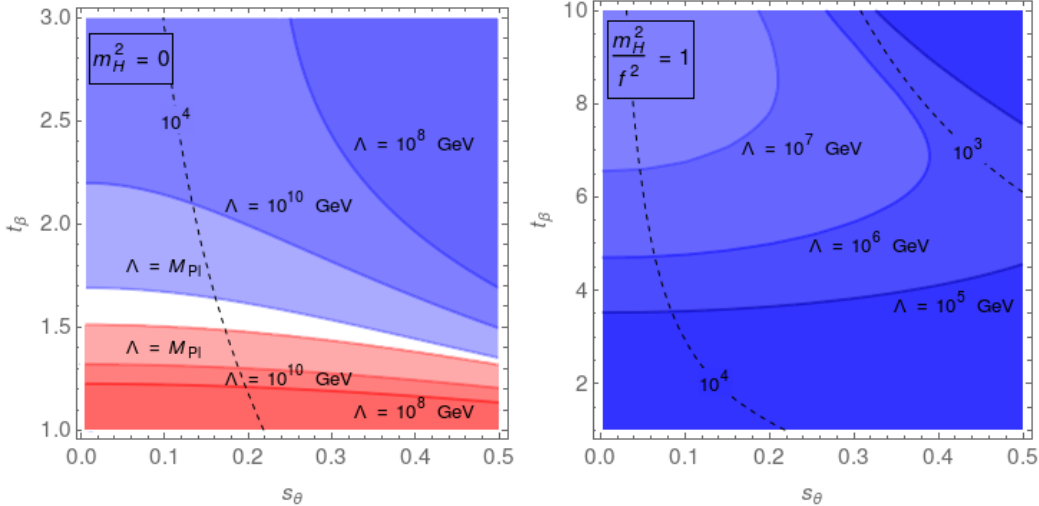
Figure 3: The blue (red) regions illustrate the vacuum instability (non-perturbativity) scale. The dashed lines show the values of $\Lambda_{\text{TC}} = 4\pi f$ in GeV. **Left panel:** $m_H^2 = 0$. On the boundaries of the regions, the vacuum is stable (couplings pertubative) up to $\Lambda = M_{\text{Pl}} = 1.22 \cdot 10^{19}$ GeV, 10^{10} GeV, 10^8 GeV. **Right panel:** $m_H^2/f^2 = 1$. On the boundaries of the regions, the vacuum is stable up to $\Lambda = 10^7$ GeV, 10^6 GeV, 10^5 GeV.

In the numerical analysis we assume that the top quark Yukawa and the EW gauge couplings run as in the SM below the condensation scale Λ_{TC}, and we neglect the threshold effects on the quartic coupling running. We fix the initial values of the SM gauge couplings at $\mu_Z = m_Z$, and the value of the SM top Yukawa from $y_t^{\text{SM}}(m_t)$ as in [25]. Furthermore, at the condensation scale, Λ_{TC}, we fix the TC gauge coupling to the estimate of the critical value [26], $\alpha_{\text{TC}}^{\text{c}} = \frac{\kappa}{C_2(R_F)}$, where $\kappa \sim \mathcal{O}(1)$, and we assume identical Yukawa couplings of the U, D technifermions $y_U(\Lambda_{\text{TC}}) = y_D(\Lambda_{\text{TC}}) \equiv y_Q^0$. However, we note that since $y_{UD} \ll 1$ throughout parameter space consistent with the vacuum and Higgs mass conditions, the contribution of the new fermions to the running of the quartic coupling is negligible.

In Fig. 3, we show the vacuum instability and perturbativity scales, $\Lambda_{\text{stab}}, \Lambda_{\text{pert}}$, resp., defined through $\lambda_H(\Lambda_{\text{stab}}) = 0$, $\lambda_H(\Lambda_{\text{pert}}) = 4\pi$, in the s_θ, t_β plane for two different values of $m_H^2/f^2 = 0$ and $m_H^2/f^2 = 1$. Small values $m_H^2/f^2 \ll 1$ correspond to large values of λ_H as is evident from the vacuum equations and yield a larger vacuum instability scale. As seen in the left panel of Fig. 3, there is a narrow window in parameter space with vacuum stability and perturbativity up to the Planck scale for relatively small t_β. For even smaller values of t_β, the quartic becomes non-perturbative, whereas for larger values of t_β the initial value of λ_H decreases, while the top coupling is still enhanced leading to vacuum instability at lower scales. Increasing m_H^2/f^2 lowers the viable values of λ_H, and this window is lost as seen in the right panel of Fig. 3.

The same increase in scale happens when s_θ is reduced with m_H^2 and t_β fixed. This corresponds to decreasing of v/f and thus from the vacuum conditions and the Higgs mass condition increasing λ_H.

Overall, demanding a stable vacuum to high scales requires tuning m_H^2/f^2 small. This implies at least a modest hierarchy between the scalar mass parameter and the compositeness scale. On the other hand, increasing the (absolute value of the) scalar mass parameter, m_H^2, with respect to the SM value requires tuning $s_\theta \ll 1$ small. This must arise from balancing two sources of unrelated physics. In Fig. 4, we show the maximum allowed values of
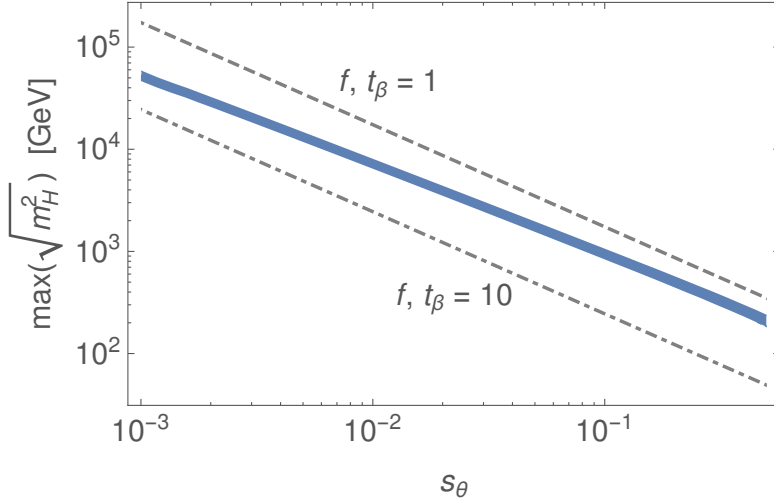
Figure 4: The blue band shows the maximum allowed value of $\sqrt{m_H^2}$ as a function of s_θ if stability at least up to the compositeness scale, $\Lambda_{\rm TC} = 4\pi f$, is required and t_β is varied within the range $1\ldots 10$. The dashed (dot-dashed) line shows f as a function of s_θ for constant value of $t_\beta = 1$ ($t_\beta = 10$).

m_H^2 as a function of s_θ demanding vacuum stability at least up to the compositeness scale, $\Lambda_{\rm TC} = 4\pi f$. This constrains the maximum possible m_H^2 regardless of the UV completion above the compositeness scale. We emphasize that while tuning $s_\theta \ll 1$ allows for larger values of m_H^2, it does not increase the maximum possible value of m_H^2/f^2. For example for $s_\theta = 0.1$, and $t_\beta = 1$ ($t_\beta = 10$) we find $\max\left(\frac{m_H^2}{f^2}\right) \approx 0.3$ (14.5), whereas for $s_\theta = 10^{-3}$, the corresponding value is 0.1 (5.7).

3.3 Additional source for the top-quark mass

As seen in the previous RG analysis, in the simplest partially composite scenarios, the top-Yukawa coupling is enhanced with respect to the SM driving the running quartic coupling to negative values before the Planck scale in most of parameter space. As seen in Fig. 3, there is a small region where the weak scale value of the quartic itself is sufficiently enhanced with respect to the SM Higgs value, to counter balance the enhanced top Yukawa. A way to reduce the constraints from vacuum stability is to assume the top quark mass is not entirely due to the elementary scalar vev, but acquires a contribution from some still unspecified dynamics. This implies a reduction of the top Yukawa coupling of σ_h in Eq. (3.5).

To this end, we start by adding a four-fermion operator between the top and the techniquarks

$$\mathcal{L}_{4\rm f} \sim -\frac{Y_t Y_U}{\Lambda_t^2}(\bar{q}_{\rm L} t_{\rm R})_\alpha^\dagger (Q^T P_\alpha Q) + \text{ h.c.} \tag{3.11}$$

We discuss the possible sources of the above four-fermion operator in the end of the section.

Upon the condensation of the techniquarks, this yields a contribution to the top mass, i.e.

$$\mathcal{L}_{4\rm f} \sim -4\pi f^3 Z_2 \frac{Y_t Y_U}{\Lambda_t^2}\text{Tr}[P_1\Sigma]\bar{t}t = -y_t' f s_\theta\,\bar{t}t + \ldots, \tag{3.12}$$

where

$$y'_t \equiv \frac{4\pi f^2 Y_t Y_U Z_2}{\Lambda_t^2}. \tag{3.13}$$

Furthermore, this gives a contribution to the effective potential via the top loop

$$V_{\text{top}} = -C_t y'^2_t f^4 \left|\text{Tr}[P_\alpha \Sigma]\right|^2 = -C_t y'^2_t f^4 s_\theta^2 + \ldots \tag{3.14}$$

Ignoring the subdominant EW-gauge contributions, the effective potential becomes

$$V_{\text{eff,top}} = V_{\text{eff}} + V_{\text{top}} \tag{3.15}$$

where V_{eff} is given in Eq. (2.9). Defining ξ_t as the fraction of the top mass originated from this new contribution,

$$y'_t f s_\theta \equiv \xi_t m_t, \tag{3.16}$$

the vacuum condition in θ is changed to

$$0 = \left.\frac{\partial V_{\text{eff,top}}}{\partial \theta}\right|_{\text{vac}} = \left.\frac{\partial V_{\text{eff}}}{\partial \theta}\right|_{\text{vac}} - \frac{2f^2 C_t \xi_t^2 m_t^2}{t_\theta}. \tag{3.17}$$

The neutral mass matrix becomes

$$M_{h,\text{top}}^2 = m_\lambda^2 \begin{pmatrix} 1 + \delta & -c_\theta t_\beta \\ -c_\theta t_\beta & t_\beta^2 + 2C_t \xi_t^2 m_t^2/m_\lambda^2 \end{pmatrix}. \tag{3.18}$$

The effect of the additional contribution to the top mass has only a tiny effect on the vacuum alignment and the scalar mass eigenvalues in most of the parameter space. Therefore, for subdominant contribution to the top mass, the main effect is just a small reduction of the top-Yukawa coupling, with Eq. (3.5) modified into

$$y_t = y_t^{\text{SM}}(1 - \xi_t)/s_\beta. \tag{3.19}$$

However, in the simplest UV-completion scenarios of the four-fermion operator, the effective treatment is valid only if the contribution to the top mass is very small.

A simple possibility to generate the four-fermion operator in Eq. (3.11) is to add an additional heavy scalar doublet that couples to the top quark and to the new fermions and can be integrated out above the compositeness scale $\Lambda_{\text{TC}} \sim 4\pi f$ [11]. Another possibility would be devising extended-technicolor (ETC) interactions [8, 9]. As opposed to ordinary TC models, ETC would only have to give a small contribution to the top mass. This would allow a higher ETC scale and thus alleviate the constraints from flavour-changing neutral currents. It would also potentially simplify the ETC construction, having only to involve the third generation as in e.g. Ref. [27]. A small reduction (at the per cent level), such as provided by a new isospin-symmetric sector giving equal mass contributions to both top and bottom and providing all of the bottom mass already soften the rapid decrease of the quartic coupling via the RG, thus enlarging the allowed range of parameter space constrained by vacuum instability. The stability plots for the value $\xi_t = m_b/m_t \simeq 0.025$ are shown in Fig. 5. The figures thus correspond to those in Fig. 3, except that part of the top mass now originates from the four-fermion operator above. The situation is in fact similar to the SM case where the uncertainty in the top mass could, in fact, bring the SM from meta-stable to stable.

3.4 Phenomenology

In this section we study constraints on the model arising from the modified Higgs couplings, from searches for new heavy scalars, and the new contributions to B-meson mixing.
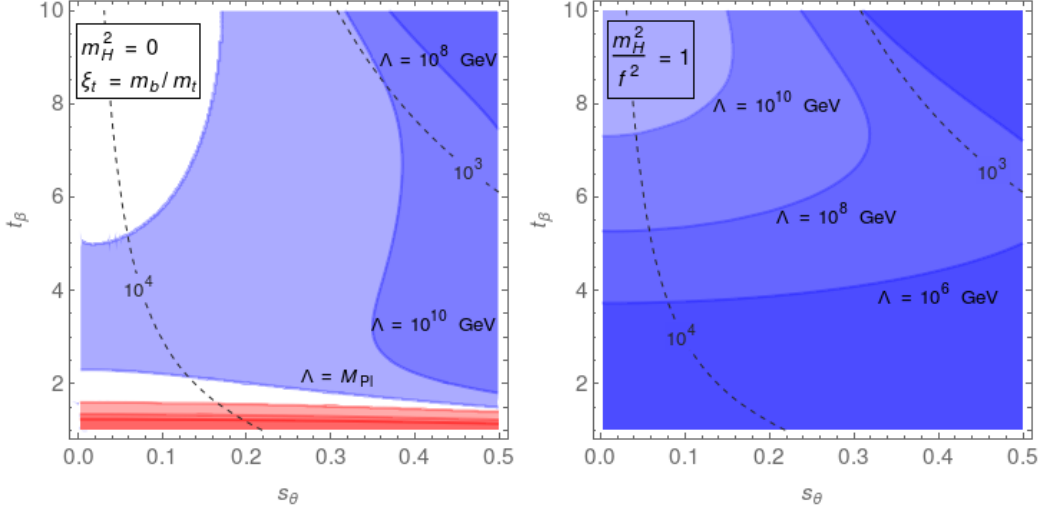
Figure 5: Corresponding plots to Fig. 3 with $\xi_t = m_b/m_t$. On the unshaded area $\Lambda \geq M_{\text{Pl}}$. The dashed lines show the values of $4\pi f$ in GeV.

3.4.1 Higgs couplings

To study the couplings of the 125-GeV Higgs state, we first define the $\kappa_{f,i}$ and $\kappa_{V,i}$ coefficients, parameterising the couplings of the mass eigenstate h_i, $i = 1, 2$ to SM fermions, f, and vector bosons, V, relative to the SM Higgs boson couplings

$$\kappa_{f,i} \equiv \frac{g_{h_i \bar{f} f}}{g_{h\bar{f} f}^{\text{SM}}}, \quad \kappa_{V,i} \equiv \frac{g_{h_i VV}}{g_{hVV}^{\text{SM}}}, \quad i = 1, 2. \tag{3.20}$$

The h_1 coefficients and their $s_\theta^2, t_\beta^{-2} \ll 1$ expansions to second order are given by

$$\begin{aligned}
\kappa_{V,1} &= c_\alpha s_\beta - s_\alpha c_\beta c_\theta \;\rightarrow\; 1 - \frac{1}{2} s_\theta^2 t_\beta^{-2}, \\
\kappa_{f,1} &= c_\alpha/s_\beta \;\rightarrow\; 1 + \frac{1}{2} s_\theta^2 t_\beta^{-2} - t_\beta^{-4} \delta \;.
\end{aligned} \tag{3.21}$$

The h_2 coefficients and their expansions to first order are given by

$$\begin{aligned}
\kappa_{V,2} &= s_\alpha s_\beta + c_\alpha c_\beta c_\theta \;\rightarrow\; \delta t_\beta^{-3}, \\
\kappa_{f,2} &= s_\alpha/s_\beta \;\rightarrow\; t_\beta^{-1} + \delta t_\beta^{-3} - \frac{1}{2} t_\beta^{-1} s_\theta^2.
\end{aligned} \tag{3.22}$$

The exact expressions above coincide with those derived in Ref. [2] and with those in a type I 2HDM except for the appearance of c_θ.

Since the 125-GeV Higgs state is identified with h_2 instead of h_1 in the small part of parameter space with $1 + \delta > t_\beta^2$ as discussed below Eq. (3.10), we use κ_f and κ_V to denote the coupling coefficients of the 125-GeV Higgs state in all of parameter space. We show the values of these coefficients in the left panel of Fig. 6 for $m_H^2 = 0$ ($\delta = 2$) together with the region disfavoured at the 2σ level by LHC measurements of the Higgs couplings from [28]. In the parameter space shown, the deviation of κ_f from unity is nearly independent of s_θ as follows from Eqs. (3.21) and (3.22) when δ is sufficiently large. In the very small t_β region, the expansions are no longer applicable.
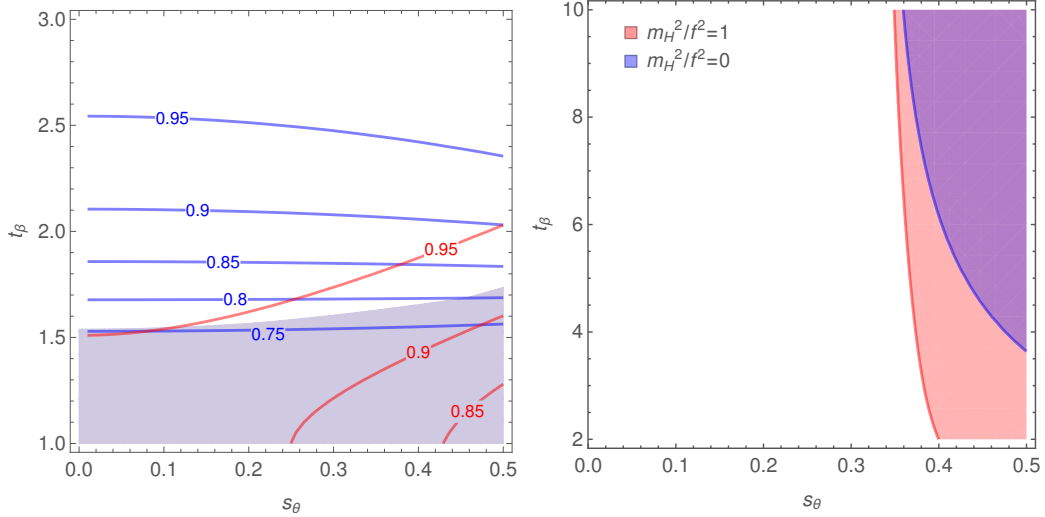
Figure 6: **Left panel:** The blue (red) curves show $|\kappa_t|$ ($|\kappa_V|$) for $m_H^2 = 0$ case. The shaded region shows the 2σ exclusion from the two-parameter κ_f, κ_V fit [28]. **Right panel:** Region in which κ_b is within 2σ of the measured value $|\kappa_b| = 0.57 \pm 0.16$, improved w.r.t. the SM prediction.

The figure demonstrates how most of the considered parameter space is still viable, but interestingly the classically scale-invariant region in Fig. 3 with vacuum stability up to the Planck scale is just above what is currently probed by LHC Higgs coupling measurements. For larger values of m_H^2 (smaller δ) the deviations from the SM value are even smaller.

In the case where we allow for a small part, ξ_t, of the top mass coming from a new sector encoded in the four-fermion interaction in Eq. (3.11), the coupling of the top quark to Higgs is only slightly further modified:

$$\kappa_t = -\xi_t \frac{s_\alpha c_\theta}{c_\beta} + (1 - \xi_t) \frac{c_\alpha}{s_\beta} \,. \tag{3.23}$$

A motivated possibility would be a new isospin-symmetric sector providing equal mass contributions to the third generation and providing all of the bottom mass. In this case $\xi_t = m_b/m_t$, and this would result in a significant modification in the couplings of the partially composite Higgs to bottom quarks:

$$\kappa_b = -\frac{s_\alpha c_\theta}{c_\beta} \,. \tag{3.24}$$

Interestingly, the measured value of this coupling by ATLAS and CMS combined is $|\kappa_b| = 0.57 \pm 0.16$ [28] and indicates a reduction of approximately 2.7σ with respect to the SM prediction according to the estimate which allows beyond-the-SM contribution in the loops. In the right panel of Fig. 6, we show the favoured region in which $|\kappa_b|$ is within the 2σ region of the measured value, for $m_H^2 = f^2$, and $m_H^2 = 0$. This reduction favours large values of s_θ, which implies a tension with the requirement of vacuum stability up to high scales.

3.4.2 Scalar production

First, we study the production of the heavier CP-even eigenstate, which we denote by $\mathcal{H}$ as above, at the LHC. Although the top coupling dominates the branching ratios parametrically, we find that the vector decay modes yield the strongest constraint. We show the

limits in Fig. 7 and find again that most of the parameter space of the model is viable. However, the LHC search for $\mathcal{H}$ production in the ZZ channel is in fact able to rule out the region stable up to the Planck scale for $m_H^2 = 0$.

The excluded cross sections at 95% CL shown in the figure correspond to analyses using collisions at 13 TeV in the center-of-mass energy to search for heavy resonances in WW/WZ production in the decay channel $\ell\nu qq$ [29] (blue), ZZ production in the decay channels $\ell^+\ell^-\ell^+\ell^-$ and $\ell^+\ell^-\nu\bar{\nu}$ [30] (orange), ZZ and ZW production in the decay channels $\ell\ell qq$ and $\nu\nu qq$ [31] (red) and Higgs boson pairs decaying into $bb\tau\tau$ [32] (green). The decays of the light Higgs have been approximated by the SM prediction. The limits are shown in dashed lines.

An interesting point to note is that the $t\bar{t}$ decay channel dominates above threshold, cf. Eq. (3.22). Resonant top-pair production is, however difficult to compute precisely due to large interference effects and QCD corrections [33–35]. The potential of the LHC experiments to observe this signal will rely on the ability to measure not only peak, but also other lineshape structures, such as peak-dip and pure dips. This search is also one of the most important programs of the LHC, since the top quark may well be related to new physics and has the least constrained interactions.

In the model an extra complication, which could in fact strengthen the signal, is the presence of near degenerate resonances: the three states, $\mathcal{H}$, π^0 and Π_5 have differences in mass of the order of few GeV, as can be seen in the left panel of Fig. 1, and thus the peak of the top pair production cross-section is expected to be enhanced—although we note that the Π_5 decays into top quarks only via higher-scale physics [36]. Top quark pair production in the CP-conserving Type-II 2HDM with degenerate masses $m_H = m_A$ and including interference effect has been considered by the ATLAS collaboration at $\sqrt{s} = 8$ TeV [37]. In the limit of small s_θ, the model here is well approximated by this case. The exclusion limit at 95% CL with $m_H = m_A = 500$ GeV is $t_\beta = 1.5$, and the exclusion limit decreases to approximately $t_\beta = 0.9$ for $m_H = m_A = 600$ GeV. At these mass values, the t_β values in the pCH models considered here are still significantly higher (cf. Fig. 1), but we expect improved results from Run II. For heavier masses, the analysis in Ref. [37] is not optimal, and the boosted regime must be considered. In Ref. [38] the LHC reach was studied for this kind of model through a reinterpretation of the top pair differential cross section measurement in both the boosted and resolved regimes. Although the near degenerate case was not considered, it seems to indicate that a very low systematic uncertainty must be achieved.

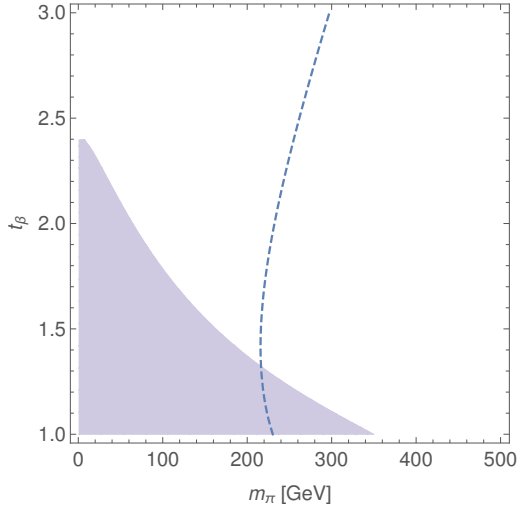### 3.4.3 $B^0 - \overline{B^0}$ mixing

Models with two Higgs doublets, including bTC models [11, 13], are in general constrained by measurements of $B^0 - \overline{B^0}$ mixing. Following [39], we calculate the contribution from the heavy pions to $B^0 - \overline{B^0}$ mixing taking into account the next-to-leading order (NLO) QCD corrections. The mass splitting can be written as

$$\Delta m_B = \frac{G_{\rm F}^2}{6\pi^2} m_W^2 |V_{td}V_{tb}^*|^2 S(x_W, x_\pi)\eta(x_W, x_\pi)B_B f_B^2 m_B, \tag{3.25}$$

where $x_{W,\pi} \equiv m_t^2/m_{W,\pi}^2$. The lengthy expressions for the functions S and η can be found in Ref. [39] and we use the current QCD lattice estimate of the decay constant $f_B\sqrt{B_B} = 216\pm10$ MeV [40]. Using the experimental result $\Delta m_B = (3.3321\pm0.0013)\cdot10^{-13}$ GeV [41], we show the 2σ exclusion region in the (m_π, t_β) plane, along with the result for the pion mass for $m_H^2 = 0$ in Fig. 8. The figure shows that the region with low $t_\beta \lesssim 1.5$ is in tension with also the $B^0 - \overline{B^0}$ results.
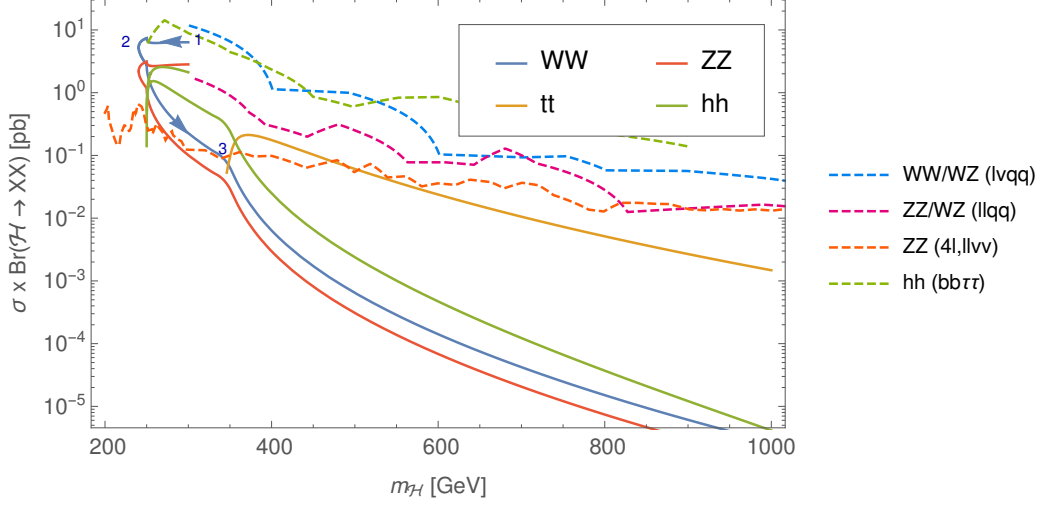
Figure 7: $\sigma \times \mathrm{Br}(\mathcal{H} \to XX)$ for the benchmark scenario with fixed $s_\theta = 0.1$ and $m_H^2 = 0$. The arrow shows the growing t_β, and the points 1, 2, and 3 represent $t_\beta = 1, 1.7, 3.6$, resp. The LHC limits are shown in dashed lines.

Figure 8: Excluded region by $B^0 - \overline{B^0}$ mixing. The dashed curve shows the value of m_π calculated for the benchmark scenario with $m_H^2 = 0$.

4 Model II: RG analysis and phenomenological constraints

We now consider the analysis of our Model II where the SU(2) doublet of elementary scalars is extended to a full SU(4) multiplet Φ. We refer to Sec. 2.2 for a short review of the model and the effective potential.

4.1 Vacuum and spectrum

Following Ref. [5], we proceed to minimize the effective potential given in Eqs. (2.13)–(2.15). This yields equations of constraint for the SU(4) invariant Yukawa coupling, y_Q,

the vev of the singlet scalar, v_S, and the SU(4)-breaking mass parameter, δm^2:

$$y_Q = \frac{m_\lambda^2 v}{8\sqrt{2}\pi Z_2 f^3 s_\theta}, \quad v_S = \frac{\widetilde{C}_g Z_2^2 f^4 s_\theta^2 - v^2 m_\lambda^2}{t_\theta v m_\lambda^2}, \quad \delta m^2 = \frac{\widetilde{C}_g Z_2^2 f^4 s_\theta^2 m_\lambda^2}{v^2 m_\lambda^2 - \widetilde{C}_g Z_2^2 f^4 s_\theta^2}, \qquad (4.1)$$

where $v \equiv \langle\sigma_h\rangle$, $v_S \equiv \langle S_\mathrm{R}\rangle$, $m_\lambda^2 \equiv m_\Phi^2 + \lambda_\Phi(v^2 + v_S^2)$, and $\widetilde{C}_g \equiv C_g(3g^2 + g'^2)$.

The three CP-even neutral states $\sigma_h, \Pi_4, S_\mathrm{R}$ mix, but with the δm^2 perturbation in the scalar potential, we do not have simple analytical formulas for the mass mixings. We therefore solve numerically the rotation matrix, R, defined by

$$\begin{pmatrix} h_1 \\ h_2 \\ h_3 \end{pmatrix} \equiv R \begin{pmatrix} \sigma_h \\ \Pi_4 \\ S_\mathrm{R} \end{pmatrix}. \qquad (4.2)$$

The lightest mass eigenstate, h_1, is identified with the observed Higgs boson with mass $m_{h_1} = 125$ GeV. The masses of the physical heavy pion triplet, $\pi^{\pm,0}$, orthogonal to those eaten by the W and Z bosons are given by

$$(m_\pi^{\pm,0})^2 = \frac{8\sqrt{2}\pi Z_2 v_\mathrm{w}^2 y_Q}{t_\beta s_\theta^2}. \qquad (4.3)$$

There are two additional CP-odd states in the spectrum: the mass eigenstates composed of Π_5 and S_I. The spectrum for fixed $s_\theta = 0.1$ is shown in Fig. 1.

As shown in [5], it is also in this model possible to achieve the EWSB driven purely by the strong dynamics with $m_\Phi^2 > 0, \delta m^2 > 0$. In particular, in the viable parameter space able to produce the correct Higgs mass, the quartic coupling is generically enhanced with respect to the SM value. Furthermore, $\delta m^2 \sim m_\Phi^2 \sim f^2$, and thus for $s_\theta \lesssim 0.1$ the scalar mass parameters reach above 1 TeV.

4.2 RG analysis

The values of the new Yukawa couplings, y_Q, for successful vacuum solutions are very small, $y_Q \ll 1$ throughout the parameter space that we consider. We therefore neglect their contributions to the one-loop β-functions of the model given in App. B.

The vacuum stability is improved with respect to Model I due to the enhanced quartic coupling, λ_Φ, in most of the parameter space. However, the extended scalar sector now plays an important role because the SM-singlet elementary scalars, $S_\mathrm{I,R}$, do not couple to SM fermions, and due to $y_Q \ll 1$ only very feebly to the techniquarks. Their quartic self-couplings may therefore develop Landau poles, and in fact the bounds on parameter space from perturbativity of these couplings are more relevant than that coming from requiring vacuum stability. We calculate the scale, Λ, at which at least one of the couplings exceeds 4π, and plot the contours of $\Lambda = M_\mathrm{Pl}$, 10^{15} GeV, 10^{12} GeV as dashed vertical lines in Fig. 9 along with the mass parameters m_Φ^2 and δm^2. Below the cyan line on the left panel of Fig. 9, $m_\Phi^2 > 0$, while $\delta m^2 > 0$ throughout, and the EWSB is completely induced by the composite sector. On the shaded gray region, the correct Higgs mass cannot be achieved. See Ref. [5] for details.

One possibility to tame the running of the quartic couplings of the EW-singlet scalars $S_\mathrm{I,R}$ is to couple these to right-handed neutrinos ν_R with $\lesssim \mathcal{O}(1)$ Yukawa couplings. This will drive the singlet quartics down, and result in higher perturbativity scale, as shown in Ref. [42] in a generic framework with one singlet scalar and singlet fermion. Interestingly, in this case one family of leptons e_L, ν_L, e_R^*, ν_R may be embedded into a full SU(4) multiplet under the global symmetry analogously to the technifermions, as done in e.g. Ref. [43]. The vev in the singlet direction would in this case give dynamical Majorana masses for the ν_R's, while the vev in the doublet direction would yield a Dirac mass term. We leave the specifics of this construction for future work.
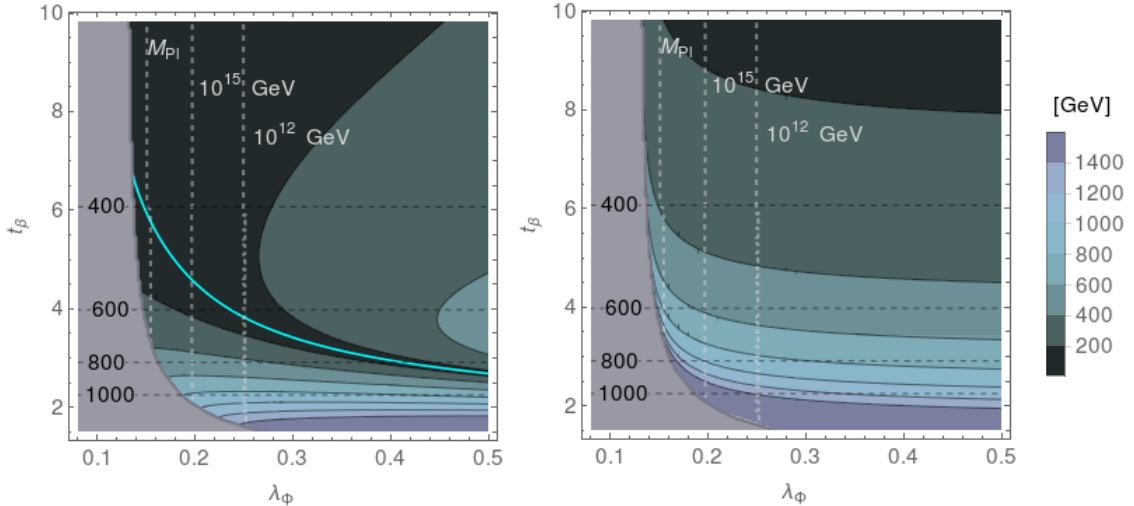
Figure 9: The values of mass parameters $\sqrt{|m_\Phi^2|}$ ($\sqrt{\delta m^2}$) are shown in left (right) panel when the Higgs mass is imposed for fixed $s_\theta = 0.1$. Below the cyan line $m_\Phi^2 > 0$, while $\delta m^2 > 0$ throughout. On the gray region on the left, no solution to the Higgs-mass constraint is found. See Ref. [5] for details. The dashed vertical lines show the parameter values where the maximum scale up to which the perturbativity of the coupligns can be attained is 10^{12} GeV, 10^{15} GeV or $M_{\rm Pl}$.

4.3 Phenomenology

The constraints from $B^0 - \overline{B^0}$ mixing are not relevant in the parameter space considered in Fig. 9 because the scalar masses are now heavy in the range where t_β is small and vice versa. The functions S and η in Eq. (3.25) are therefore always small. The κ-coefficients for this model, defined as in Eq. (3.20) but now with $i = 1, 2, 3$, can be written in terms of the rotation matrix defined in Eq. (4.2) as

$$\kappa_{f,i} = \frac{R_{i1}}{s_\beta}, \quad \kappa_{V,i} = R_{i1}s_\beta + R_{i2}c_\beta c_\theta, \quad i = 1, 2, 3. \tag{4.4}$$

We refer to Ref. [5] for an explicit illustration of the $\kappa_{f,1}$-coefficient for fixed value of $s_\theta = 0.1$. We conclude that for the most of the parameter space, the model is within the 2σ region of two-parameter fit of $\kappa_{f,1}, \kappa_{V,1}$ on the combined CMS+ATLAS Run 1 data [28].

We present the collider limits relevant to the next to lightest neutral CP-even scalar, h_2, in Fig. 10. The constraint from searches for heavy neutral scalars in the ZZ channel is reduced as compared to the SU(2)-doublet-scalar case due to the additional mixing with the singlet $S_{\rm R}$. At face value, disregarding the fluctuations at small masses, the limit is about 225 GeV. In particular we note that the top coupling is significantly suppressed as compare to the Model I, and even at large mass the $t\bar{t}$ production is subdominant.

On the other hand, the π^0 and h_3 states decay almost exclusively to $t\bar{t}$ for $s_\theta \lesssim 0.1$ as can be seen in the branching ratio to $t\bar{t}$ shown in Fig. 11c (off-shell decays were neglected in the figure). At larger values of s_θ, the masses can get lower than the $t\bar{t}$ threshold, $m_{\pi^0} < 2m_t$, and other decay channels become important, cf. Fig. 11a. In the case of h_3, the opening of other channels is more severe since it couples at tree level to weak bosons and to di-Higgs. For the π^0 state, the Zh channel becomes dominant.
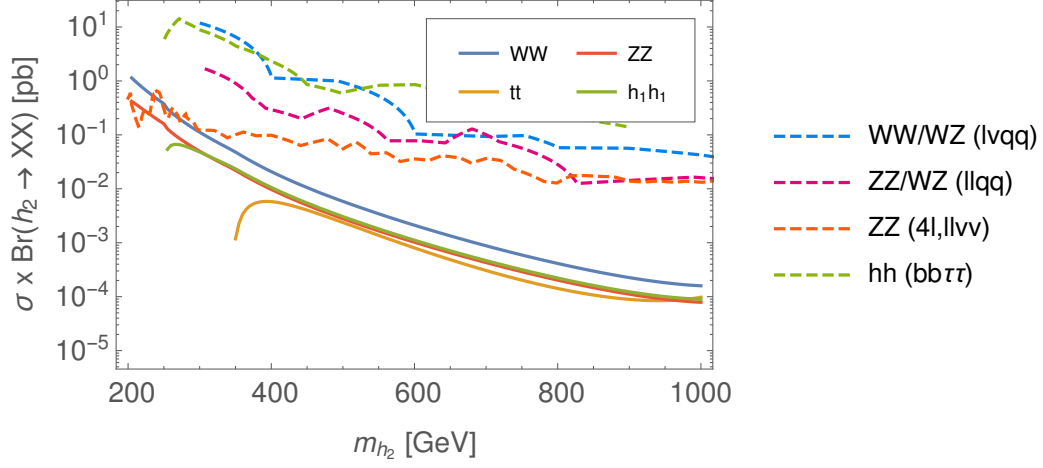
Figure 10: $\sigma \times \mathrm{Br}(h_2 \to XX)$ in different channels with corresponding collider limits. We have fixed $\lambda_\Phi = 0.15$ and $s_\theta = 0.1$.

(a)

(b)

(c)
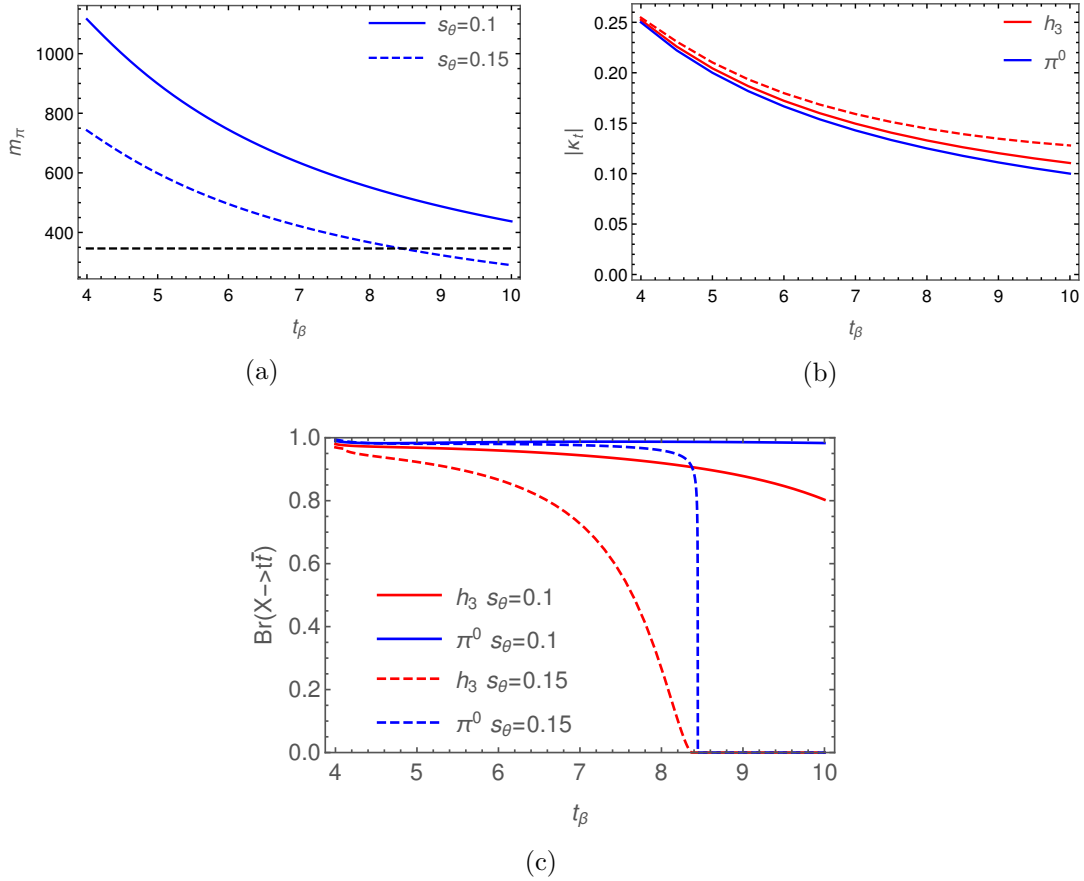
Figure 11: (a) Mass of the π^0. The dashed horizontal line shows the $t\bar{t}$ threshold. (b) Reduced coupling to top quarks. (c) Branching ratio of h_3 and π^0 to top-quark pair. In all panels $\lambda_\Phi = 0.15$ and $s_\theta = 0.1$ (0.15) in the solid (dashed) lines.

In the case where the top decay channel prevails, we can have a situation in which the LHC might be able to observe these states. To see this, we first note that these states are nearly degenerate in mass (see Fig. 1) and therefore they would be seen as a single summed peak at the LHC detectors. To access the magnitude of the peaks, we further note that the coupling of both states to top quarks are very similar, and thus also their total widths (in the case of top dominated) as can be seen in Fig. 11b (the variation with λ_ϕ is very small). Therefore, the production of both resonances can be effectively parametrized by the sum of the couplings. The magnitude of this sum could be within the expected reach of LHC, even for heavy masses, if the systematic uncertainty in $t\bar{t}$ can be mildly improved [38].

5   Conclusions

In this paper, we have studied the phenomenology of partially composite Higgs models based on the coset $SU(4)/Sp(4)$. In particular, we have considered the constraints on their parameter space from vacuum stability and perturbativity of the scalar self-couplings, together with constraints coming from Higgs coupling measurements, $B^0 - \overline{B^0}$ mixing and LHC searches for new heavy scalars.

We considered two realisations of the elementary scalar sector: a minimal one with a single EW doublet coupled to the new fermions, and one with an $SU(4)$ multiplet of scalars. In both models the new fermions feature vector-like current masses needed for the proper vacuum alignment; in the latter model they are dynamically generated by a vev of a EW-singlet component of the $SU(4)$ scalar multiplet.

We have shown that in the minimal model there exists a region of allowed parameter values such that the vacuum remains stable and couplings perturbative up to the Planck scale. The EWSB is induced dynamically via the condensation in the strongly-interacting new fermion sector. However, it is only possible to push the value of the mass parameter of the elementary scalar towards the compositeness scale $\Lambda = 4\pi f$, and not beyond, at the expense of a lower vacuum stability scale. If we require stability of the vacuum up to the compositeness scale we find a bound on the mass parameter which is roughly $m_H^2 \lesssim (0.1\, s_\theta^{-1}\, \mathrm{TeV})^2$. Conversely, the parameter region with vacuum stability up to the Planck scale lies near the classically scale-invariant region. However, we also show that LHC searches for new heavy CP-even scalars exclude this narrow stable window, while the constraints from a global fit to LHC Higgs coupling measurements and $B^0 - \overline{B^0}$ mixing measurements are just beginning to probe this part of parameter space.

In summary, in most of the parameter space of the minimal model, the vacuum becomes unstable before the Planck scale due to the enhanced top-Yukawa coupling of the elementary scalar as compared to the SM Higgs. This issue can be alleviated, if the top quark acquires a small part of its mass, e.g. of the order of the b-quark mass, from some other source than the elementary scalar. One such source could be ETC-type four-fermion operators. However, large modifications in the bottom-Higgs coupling would then lead to tension with the measurements in the stability region.

The second model with a full $SU(4)$ multiplet of scalars allows for dynamical generation of the vector-like masses of the new fermions, and the required explicit breaking of the $SU(4)$ symmetry can be in the scalar potential as opposed to the Yukawa couplings in the minimal model. The quartic scalar couplings are in general enhanced compared to the SM removing the vacuum stability issue. However, due to the non-minimal scalar content, the singlet-scalar couplings instead develop Landau poles before the Planck scale in part of the parameter space. Again this limits the scalar mass parameters to the TeV region. One possibility to alleviate this problem is coupling the EW-singlet scalars to right-handed neutrinos. This model is also less constrained by current LHC searches and $B^0 - \overline{B^0}$ mixing, but the top decay channel might provide an interesting possibility to observe the heavier scalar states of the model at the LHC in the future.

Acknowledgments

A RG equations: elementary doublet

We consider a rather generic bTC framework featuring N_F new $SU(2)_L$-doublet fermionic fields, $Q_L = (U_L, D_L)$, transforming under the representation R_F under the new strong gauge group, and coupling to the elementary Higgs doublet via Yukawa interactions. The one-loop evolution of the relevant couplings above the condensation scale, Λ_{TC}, is given by

$$16\pi^2 \beta_{g_c} = -7g_c^3,$$

$$16\pi^2 \beta_{g_{TC}} = -\left(\frac{11}{3}C_2(A) - \frac{8}{3} \cdot N_F T(R_F)\right) g_{TC}^3,$$

$$16\pi^2 \beta_{g_L} = -\left(\frac{19}{6} - \frac{2}{3} N_F d(R_F) T(R_F)\right) g_L^3,$$

$$16\pi^2 \beta_{g_Y} = \left(\frac{41}{6} + \frac{4}{3} N_F d(R_F) \left(4Y(Q_L)^2 + \frac{1}{2}\right)\right) g_Y^3,$$

$$16\pi^2 \beta_{y_t} = \left(-8g_c^2 - \frac{9}{4}g_L^2 - \frac{17}{12}g_Y^2 + \frac{9}{2}y_t^2 + d(R_F)(y_U^2 + y_D^2)\right) y_t,$$

$$16\pi^2 \beta_{y_U} = \left(-6C_2(R_F)g_{TC}^2 - \frac{9}{4}g_L^2 - \frac{17}{12}g_Y^2 + 3y_t^2 + \left(d(R_F) + \frac{3}{2}\right) y_U^2 + d(R_F)y_D^2\right) y_U,$$

$$16\pi^2 \beta_{y_D} = \left(-6C_2(R_F)g_{TC}^2 - \frac{9}{4}g_L^2 - \frac{5}{12}g_Y^2 + 3y_t^2 + \left(d(R_F) + \frac{3}{2}\right) y_D^2 + d(R_F)y_U^2\right) y_D,$$

$$16\pi^2 \beta_\lambda = 24\lambda^2 + \lambda\left(-3\left(3g_L^2 + g_Y^2\right) + 12y_t^2 + 4d(R_F)\left(y_U^2 + y_D^2\right)\right)$$
$$+ \frac{3}{8}\left(2g_L^4 + \left(g_L^2 + g_Y^2\right)^2\right)\right) - 6y_t^4 - 2d(R_F)(y_U^4 + y_D^4),$$

$$\tag{A.1}$$

where

$$\beta_g \equiv \frac{\mathrm{d}g}{\mathrm{d}\log\mu}, \tag{A.2}$$

$T(R_F)$ and $d(R_F)$ are the index and dimension of the representation R_F, and $C_2(A)$ is the quadratic Casimir of the adjoint representation.

B RG equations: $SU(4)$ multiplet of elementary scalars

Here we write down the RG equations for specific bTC framework based on $SU(4)/Sp(4)$ coset described in the main text. The new $SU(2)_L$-doublet fermionic fields, $Q_L = (U_L, D_L)$, transform in the fundamental representation of the new strong gauge group, and couple to the multiplet of elementary scalars transforming in the two-index antisymmetric representation of $SU(4)$ via Yukawa interactions. From the RG point of view, the scalar sector corresponds to an EW doublet and two singlets, and the $SU(4)$ invariance of the potential can be achieved only for one renormalisation scale μ_0. The quartic scalar potential can be written as

$$V^{(4)} = \lambda_H(H^\dagger H)^2 + \frac{\lambda_{S_R}}{4}S_R^4 + \frac{\lambda_{S_I}}{4}S_I^4 + \lambda_{HS_R}(H^\dagger H)S_R^2 + \lambda_{HS_I}(H^\dagger H)S_I^2 + \frac{\lambda_{S_R S_I}}{2}S_R^2 S_I^2, \tag{B.1}$$

with $SU(4)$-symmetric boundary values $\lambda_H(\mu_0) = \lambda_{S_R}(\mu_0) = \lambda_{S_I}(\mu_0) = \lambda_{HS_R}(\mu_0) = \lambda_{HS_I}(\mu_0) = \lambda_{S_R S_I}(\mu_0) = \lambda_\Phi$.

The one-loop evolution of the relevant couplings above the condensation scale, Λ_{TC}, is given by (we ignore the new Yukawa couplings, since for the viable parameter points able

to give the correct Higgs mass, $y_Q \lesssim 0.1$ throughout the parameter space we consider, and are thus their contribution to the β-functions is completely subdominant)

$$16\pi^2\beta_{g_{\mathrm{TC}}} = -6g_{\mathrm{TC}}^3, \quad 16\pi^2\beta_{g_{\mathrm{L}}} = -\frac{5}{2}g_{\mathrm{L}}^3, \quad 16\pi^2\beta_{g_Y} = \frac{15}{2}g_Y^3,$$

$$16\pi^2\beta_{y_t} = \left(-8g_c^2 - \frac{9}{4}g_{\mathrm{L}}^2 - \frac{17}{12}g_Y^2 + \frac{9}{2}y_t^2\right)y_t,$$

$$16\pi^2\beta_{\lambda_H} = 24\lambda_H^2 + 2(\lambda_{HS_R}^2 + \lambda_{HS_I}^2) + \lambda_H\left(-3\left(3g_{\mathrm{L}}^2 + g_Y^2\right) + 12y_t^2\right)$$
$$+ \frac{3}{8}\left(2g_{\mathrm{L}}^4 + \left(g_{\mathrm{L}}^2 + g_Y^2\right)^2\right)\right) - 6y_t^4,$$

$$16\pi^2\beta_{\lambda_{HS_R}} = 8\lambda_{HS_R}^2 + 6\left(2\lambda_H + \lambda_{S_R}\right)\lambda_{HS_R} + 2\lambda_{HS_I}\lambda_{S_RS_I}$$
$$+ \lambda_{HS_R}\left(-\frac{3}{2}\left(3g_{\mathrm{L}}^2 + g_Y^2\right) + 6y_t^2\right), \tag{B.2}$$

$$16\pi^2\beta_{\lambda_{HS_I}} = 8\lambda_{HS_I}^2 + 6\left(2\lambda_H + \lambda_{S_I}\right)\lambda_{HS_I} + 2\lambda_{HS_R}\lambda_{S_RS_I}$$
$$+ \lambda_{HS_I}\left(-\frac{3}{2}\left(3g_{\mathrm{L}}^2 + g_Y^2\right) + 6y_t^2\right),$$

$$16\pi^2\beta_{\lambda_{S_R}} = 18\lambda_{S_R}^2 + 8\lambda_{HS_R}^2 + 2\lambda_{S_RS_I}^2,$$

$$16\pi^2\beta_{\lambda_{S_I}} = 18\lambda_{S_I}^2 + 8\lambda_{HS_I}^2 + 2\lambda_{S_RS_I}^2,$$

$$16\pi^2\beta_{\lambda_{S_RS_I}} = 8\lambda_{S_RS_I}^2 + 6\lambda_{S_RS_I}(\lambda_{S_R} + \lambda_{S_I}) + 8\lambda_{HS_R}\lambda_{HS_I}.$$

References

[1] D. B. Kaplan and H. Georgi, *SU(2) × U(1) Breaking by Vacuum Misalignment, Phys.Lett.* **B136** (1984) 183.

[2] J. Galloway, A. L. Kagan, and A. Martin, *A UV complete partially composite-pNGB Higgs, Phys. Rev.* **D95** (2017), no. 3 035038, [arXiv:1609.05883].

[3] A. Agugliaro, O. Antipin, D. Becciolini, S. De Curtis, and M. Redi, *UV complete composite Higgs models, Phys. Rev.* **D95** (2017), no. 3 035019, [arXiv:1609.07122].

[4] T. Alanne, M. T. Frandsen, and D. Buarque Franzosi, *Testing a dynamical origin of Standard Model fermion masses, Phys. Rev.* **D94** (2016) 071703, [arXiv:1607.01440].

[5] T. Alanne, D. Buarque Franzosi, and M. T. Frandsen, *A partially composite Goldstone Higgs, Phys. Rev.* **D96** (2017) 095012, [arXiv:1709.10473].

[6] G. 't Hooft, *Naturalness, chiral symmetry, and spontaneous chiral symmetry breaking, NATO Sci. Ser. B* **59** (1980) 135.

[7] D. B. Kaplan, *Flavor at SSC energies: A New mechanism for dynamically generated fermion masses, Nucl. Phys.* **B365** (1991) 259–278.

[8] E. Eichten and K. D. Lane, *Dynamical Breaking of Weak Interaction Symmetries, Phys. Lett.* **B90** (1980) 125–130.

[9] S. Dimopoulos and L. Susskind, *Mass Without Scalars, Nucl. Phys.* **B155** (1979) 237–252.

[10] D. B. Kaplan, H. Georgi, and S. Dimopoulos, *Composite Higgs Scalars, Phys.Lett.* **B136** (1984) 187.

[11] E. H. Simmons, *Phenomenology of a Technicolor Model With Heavy Scalar Doublet, Nucl.Phys.* **B312** (1989) 253.

[12] A. Kagan and S. Samuel, *The Family mass hierarchy problem in bosonic technicolor, Phys. Lett.* **B252** (1990) 605–610.

[13] C. D. Carone, *Technicolor with a 125 GeV Higgs Boson*, *Phys.Rev.* **D86** (2012) 055011, [arXiv:1206.4324].

[14] G. Ferretti and D. Karateev, *Fermionic UV completions of Composite Higgs models*, *JHEP* **03** (2014) 077, [arXiv:1312.5330].

[15] R. Lewis, C. Pica, and F. Sannino, *Light Asymmetric Dark Matter on the Lattice: SU(2) Technicolor with Two Fundamental Flavors*, *Phys. Rev.* **D85** (2012) 014504, [arXiv:1109.3513].

[16] M. A. Luty and T. Okui, *Conformal technicolor*, *JHEP* **09** (2006) 070, [hep-ph/0409274].

[17] J. Galloway, J. A. Evans, M. A. Luty, and R. A. Tacchi, *Minimal Conformal Technicolor and Precision Electroweak Tests*, *JHEP* **1010** (2010) 086, [arXiv:1001.1361].

[18] G. Cacciapaglia and F. Sannino, *Fundamental Composite (Goldstone) Higgs Dynamics*, *JHEP* **04** (2014) 111, [arXiv:1402.0233].

[19] D. Buarque Franzosi, G. Cacciapaglia, H. Cai, A. Deandrea, and M. Frandsen, *Vector and Axial-vector resonances in composite models of the Higgs boson*, *JHEP* **11** (2016) 076, [arXiv:1605.01363].

[20] S. Weinberg, *Implications of Dynamical Symmetry Breaking*, *Phys.Rev.* **D13** (1976) 974–996.

[21] L. Susskind, *Dynamics of Spontaneous Symmetry Breaking in the Weinberg-Salam Theory*, *Phys.Rev.* **D20** (1979) 2619–2625.

[22] R. Arthur, V. Drach, M. Hansen, A. Hietanen, C. Pica, and F. Sannino, *SU(2) gauge theory with two fundamental flavors: A minimal template for model building*, *Phys. Rev.* **D94** (2016), no. 9 094507, [arXiv:1602.06559].

[23] M. E. Peskin, *The Alignment of the Vacuum in Theories of Technicolor*, *Nucl. Phys.* **B175** (1980) 197–233.

[24] J. Preskill, *Subgroup Alignment in Hypercolor Theories*, *Nucl. Phys.* **B177** (1981) 21–59.

[25] G. Degrassi, S. Di Vita, J. Elias-Miro, J. R. Espinosa, G. F. Giudice, G. Isidori, and A. Strumia, *Higgs mass and vacuum stability in the Standard Model at NNLO*, *JHEP* **08** (2012) 098, [arXiv:1205.6497].

[26] W. J. Marciano, *Exotic New Quarks and Dynamical Symmetry Breaking*, *Phys. Rev.* **D21** (1980) 2425.

[27] G. Cacciapaglia and F. Sannino, *An Ultraviolet Chiral Theory of the Top for the Fundamental Composite (Goldstone) Higgs*, *Phys. Lett.* **B755** (2016) 328–331, [arXiv:1508.00016].

[28] **ATLAS, CMS** Collaboration, G. Aad et al., *Measurements of the Higgs boson production and decay rates and constraints on its couplings from a combined ATLAS and CMS analysis of the LHC pp collision data at $\sqrt{s} = 7$ and 8 TeV*, *JHEP* **08** (2016) 045, [arXiv:1606.02266].

[29] **ATLAS** Collaboration, T. A. collaboration, *Search for WW/WZ resonance production in $\ell\nu qq$ final states in pp collisions at $\sqrt{s} = 13$ TeV with the ATLAS detector*, .

[30] **ATLAS** Collaboration, T. A. collaboration, *Search for heavy ZZ resonances in the $\ell^+\ell^-\ell^+\ell^-$ and $\ell^+\ell^-\nu\bar{\nu}$ final states using proton–proton collisions at $\sqrt{s} = 13$ TeV with the ATLAS detector*, .

[31] **ATLAS** Collaboration, M. Aaboud et al., *Searches for heavy ZZ and ZW resonances in the $\ell\ell qq$ and $\nu\nu qq$ final states in pp collisions at $\sqrt{s} = 13$ TeV with the ATLAS detector*, arXiv:1708.09638.

[32] **CMS** Collaboration, A. M. Sirunyan et al., *Search for Higgs boson pair production in events with two bottom quarks and two tau leptons in proton-proton collisions at sqrt(s) = 13 TeV*, arXiv:1707.02909.

[33] W. Bernreuther, P. Galler, C. Mellein, Z. G. Si, and P. Uwer, *Production of heavy Higgs bosons and decay into top quarks at the LHC*, *Phys. Rev.* **D93** (2016), no. 3 034032, [arXiv:1511.05584].

[34] B. Hespel, F. Maltoni, and E. Vryonidou, *Signal background interference effects in heavy scalar production and decay to a top-anti-top pair*, *JHEP* **10** (2016) 016, [arXiv:1606.04149].

[35] D. Buarque Franzosi, E. Vryonidou, and C. Zhang, *Scalar production and decay to top quarks including interference effects at NLO in QCD in an EFT approach*, *JHEP* **10** (2017) 096, [arXiv:1707.06760].

[36] A. Arbey, G. Cacciapaglia, H. Cai, A. Deandrea, S. Le Corre, and F. Sannino, *Fundamental Composite Electroweak Dynamics: Status at the LHC*, *Phys. Rev.* **D95** (2017), no. 1 015028, [arXiv:1502.04718].

[37] **ATLAS** Collaboration, M. Aaboud et al., *Search for Heavy Higgs Bosons A/H Decaying to a Top Quark Pair in pp Collisions at $\sqrt{s} = 8$ TeV with the ATLAS Detector*, *Phys. Rev. Lett.* **119** (2017), no. 19 191803, [arXiv:1707.06025].

[38] D. Buarque Franzosi, F. Fabbri, and S. Schumann, *Constraining scalar resonances with top-quark pair production at the LHC*, arXiv:1711.00102.

[39] J. Urban, F. Krauss, U. Jentschura, and G. Soff, *Next-to-leading order QCD corrections for the B0 anti-B0 mixing with an extended Higgs sector*, *Nucl. Phys.* **B523** (1998) 40–58, [hep-ph/9710245].

[40] **ETM** Collaboration, N. Carrasco et al., *B-physics from $N_f = 2$ tmQCD: the Standard Model and beyond*, *JHEP* **03** (2014) 016, [arXiv:1308.1851].

[41] **Particle Data Group** Collaboration, C. Patrignani et al., *Review of Particle Physics*, *Chin. Phys.* **C40** (2016), no. 10 100001.

[42] T. Alanne, K. Tuominen, and V. Vaskonen, *Strong phase transition, dark matter and vacuum stability from simple hidden sectors*, *Nucl. Phys.* **B889** (2014) 692–711, [arXiv:1407.0688].

[43] R. Foadi, M. T. Frandsen, T. A. Ryttov, and F. Sannino, *Minimal Walking Technicolor: Set Up for Collider Physics*, *Phys.Rev.* **D76** (2007) 055005, [arXiv:0706.1696].